JMEPEG (2012) 21:2587–2593
DOI: 10.1007/s11665-012-0317-x

1059-9495/$19.00

Mechanical Behavior of Shape Memory Alloys Under Complex Loading Conditions of Stress, Strain, and Temperature

H. Cho, A. Suzuki, T. Yamamoto, and T. Sakuma

(Submitted March 7, 2012; in revised form July 5, 2012)

The transformation behavior of shape memory alloys is simulated for complex loadings of stress, strain, and temperature. Calculations are made by using the "Accommodation Model" which is a constitutive model for shape memory alloys considering the accommodation behavior of the transformation strain. Calculated results are given for the superelastic behavior, the shape memory effect, the transformation behavior under temperature change with stress or strain holding, the structural behavior of a shape memory wire with a bias spring, etc. The effect of the plastic strain on the transformation strain is also investigated.

Keywords accommodation behavior, constitutive equation, shape memory alloy, transformation

1. Introduction

In recent years shape memory alloys came to be used in mechanical components of high performance. To evaluate the deformation behavior of such components it is indispensable to develop a constitutive model which can describe the transformation behavior of shape memory alloys under various thermo-mechanical conditions. It is essential for a constitutive model of shape memory alloys to describe the accommodation mechanism which acts during phase transformation procedure. There are a lot of constitutive models developed by Tanaka (Ref 1), Tokuda (Ref 2), Brinson (Ref 3, 4), etc. which can successfully describe transformation behavior of shape memory alloys. But most of them are phenomenological ones with internal variables through which the accommodation mechanism is reflected in the models indirectly and there are few models that can directly treat the accommodation mechanism which controls transformation behaviors of microstructures of shape memory alloys. The accommodation mechanism automatically chooses transformation planes and directions which should be active so that the internal stress caused by transformation becomes smallest. One of such models that can treat the accommodation mechanism directly was developed by the authors (Ref 5, 6) and named as "accommodation model" where the equal strain assumption is employed to describe the accommodation behavior in microscopic transformation systems of crystals. An extended version of the model was also presented to incorporate the plastic deformation in addition to the transformation strain (Ref 7).

In the present paper, the outline of the proposed constitutive model is described and results of sample calculations by the constitutive model are given in order to demonstrate the ability of the model for describing the deformation behavior of shape memory alloys.

2. Constitutive Model

2.1 Outline of the Constitutive Model for Transformation

A constitutive model was proposed by the authors (Ref 5, 6) to describe the inelastic behavior of shape memory alloys such as Ti-Ni alloys where the main mechanism of the inelastic behavior is the phase transformation under thermo-mechanical conditions. In the constitutive model, a material point is treated as an aggregate of many microcrystal grains with arbitrary crystal orientations. Each grain has 24 transformation systems (transformation plane and transformation direction) which are peculiar to the crystal structure of the grain. The equal strain assumption is used in the model to connect the stress-strain relations of a material point to those of micrograins. Namely, the microscopic strain of each grain is equal to that of the macroscopic strain of the material. And the macroscopic stress is represented as the average of stresses of grains. By using this model, the compatibility of strains of grains is automatically held in the material point. Figure 1 schematically shows the equal strain model. The idea of the equal strain model has been employed before in the modified fraction model (Ref 8) for the inelastic (viscoplastic) behavior of metals under high temperatures and also is similar to that employed in the Taylor's model (Ref 9) for the plastic behavior of polycrystalline metals.

It is essential for a constitutive model to describe the accommodation mechanism in the phase transformation process of shape memory alloys. The equal strain model can successfully describe this mechanism. As the equal strain model is

This article is an invited paper selected from presentations at the International Conference on Shape Memory and Superelastic Technologies 2011, held November 6-9, 2011, in Hong Kong, China, and has been expanded from the original presentation.

H. Cho, A. Suzuki, T. Yamamoto, and **T. Sakuma,** Oita University, Oita, Oita, Japan. Contact e-mail: as-suzuki@muf.biglobe.ne.jp.

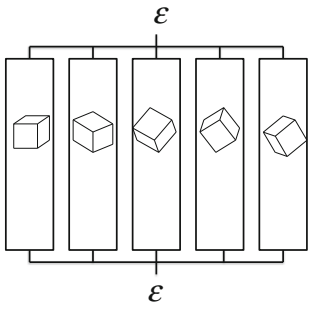

Fig. 1 Equal strain model for micrograins

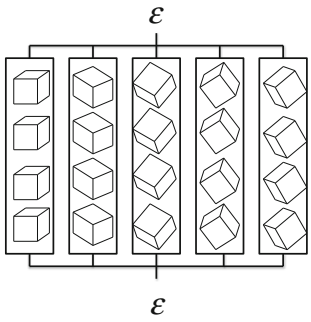

Fig. 2 Combined model of equal strain model and equal stress model for micrograins with sub-elements

applied to transformation systems of each grain and the transformation occurs in one of the transformation systems which is located in the mechanically most favorite orientation to transform, the stress relaxation occurs in that direction and one of other transformation systems becomes to be the most favorite to transform at a next loading step. The accommodation mechanism can be described in this way.

Moreover it is assumed that each micrograin is composed of many sub-elements which are in equal stress state (equal stress model or series model). And reflecting the structural variations, the critical condition for the transformation of sub-elements of a grain is assumed to be different each other to describe the work hardening in the stress-strain curve for transformation. This treatment is also shown to be useful for preventing the instability in calculation procedure, which may be caused by the onset at a time of large intrinsic transformation strains. So the constitutive model mentioned here can be called as a combined model where the equal strain model and the equal stress model are combined. The whole image of the constitutive model is schematically shown in Fig. 2.

2.2 Mathematical Formulation of Constitutive Model

It is assumed that the material is consisted of M crystal grains with different crystal orientations and a grain is divided into N sub-elements. The stress-strain relations defined in the macroscopic coordinate system are given as follows by referring to Fig. 2.

$$\sigma_{kl} = \left(\sum_{m=1}^{M} F_m \bar{C}_{ijkl,m}\right)\varepsilon_{ij} - \sum_{m=1}^{M} F_m \bar{C}_{ijkl,m}\varepsilon^{tr}_{ij,m}, \quad \text{(Eq 1)}$$

where σ_{kl} stress tensor of a material point, ε_{ij} strain tensor of a material point, $\varepsilon_{ij,m}$ strain tensor of mth grain, $\varepsilon^{e}_{ij,m}$ elastic strain tensor of mth grain, $\varepsilon^{tr}_{ij,m}$ transformation strain tensor of mth grain, F_m volume fraction of mth grain, and $\bar{C}_{ijkl,m}$ average elastic modulus tensor of mth grain.

Following relations by the equal strain hypothesis are used in deriving Eq 1.

$$\varepsilon_{ij} = \varepsilon_{ij,m} \quad \text{(Eq 2)}$$

$$\varepsilon_{ij,m} = \varepsilon^{e}_{ij,m} + \varepsilon^{tr}_{ij,m} \quad \text{(Eq 3)}$$

Transformation strain of mth grain is assumed to be the average value of transformation strains of sub-elements as

$$\varepsilon^{tr}_{ij,m} = \sum_{n=1}^{N} f_{mn}\varepsilon^{tr}_{ij,mn}, \quad \text{(Eq 4)}$$

where $\varepsilon^{tr}_{ij,mn}$ transformation strain of nth sub-element of mth grain and f_{mn} volume fraction of nth sub-element of mth grain.

Average elastic modulus tensor of mth grain is represented as

$$\bar{C}_{ijkl,m} = \sum_{n=1}^{N} f_{mn} C_{ijkl,mn}, \quad \text{(Eq 5)}$$

where $C_{ijkl.mn}$ is elastic modulus tensor of nth sub-element of mth grain.

Elastic modulus tensor is assumed to be isotropic in the present paper. Also, following equations are given

$$\sum_{m=1}^{M} F_m = 1 \quad \text{(Eq 6)}$$

$$\sum_{n=1}^{N} f_{mn} = 1 \quad \text{(Eq 7)}$$

An inverse relation of Eq 1 is given as

$$\varepsilon_{ij} = \left(\sum_{m=1}^{M} F_m \bar{C}_{ijkl,m}\right)^{-1}\sigma_{kl} + \left(\sum_{m=1}^{M} F_m \bar{C}_{ijkl,m}\right)^{-1} \times \sum_{m=1}^{M} F_m \bar{C}_{ijkl,m}\varepsilon^{tr}_{ij,m} \quad \text{(Eq 8)}$$

2.3 Calculation Procedure to Obtain Stress of Material Point Under Given Strain of Material Point

When the (total) strain of a material point is given, the stress of the material point can be calculated as below. By the assumption of equal strain, the strain of the grain is equal to the strain of the material point. The elastic strain of each grain is obtained by subtraction of the transformation strain from the total strain of the grain, and by multiplying the elastic strain of each grain with the elastic constant considering the volume fractions of each phase, the stress of each grain is calculated. According to the assumption of the equal stress, the stress thus calculated is applied to all sub-elements of a grain. The resolved shear stress acting on each transformation system of each sub-element is calculated, and when the maximum value of the resolved shear stress becomes larger than the critical value, the transformation occurs in its transformation system and the intrinsic transformation strain value is given to the sub-element. Considering the volume fraction of the sub-element,

the average value of transformation strains of sub-elements is given as the transformation strain of the grain. The stress of a material point is the average value of stress of all grains with volume fractions.

2.4 Intrinsic Transformation Strain

The intrinsic transformation strains are given for the transformation system with the transformation plane perpendicular to the third coordinate axis and the transformation direction parallel to the first coordinate axis as

$$\tilde{\varepsilon}^* = \begin{bmatrix} 0 & 0 & \tilde{\gamma}/2 \\ 0 & 0 & 0 \\ \tilde{\gamma}/2 & 0 & \tilde{\varepsilon} \end{bmatrix}, \qquad \text{(Eq 9)}$$

and sample values for Cu-Zn-Sn shape memory alloy has been presented in Ref 10 as

$$\tilde{\gamma} = 0.2, \quad \tilde{\varepsilon} = -0.004 \qquad \text{(Eq 10)}$$

This equation shows that the normal component of the intrinsic transformation strain is not so large. So, referring to Eq 10, values of

$$\tilde{\gamma} = 0.2, \quad \tilde{\varepsilon} = 0 \qquad \text{(Eq 11)}$$

are employed for simplicity in the present study. But when the accommodation behavior is evaluated for the case of the thermal-induced transformation under stress-free conditions, normal component should be taken into consideration (Ref 6).

2.5 Critical Conditions for Transformation (Ref 5, 6)

The transformation of shape memory alloys is mainly controlled by the resolved shear stress on the transformation plane. Here it is assumed that the transformation will occur when the resolved shear stress on the transformation plane equals to its critical value. Denoting the resolved shear stress as τ and the critical value of it as τ_M, the condition for the transformation is represented as

$$\tau = \tau_M \qquad \text{(Eq 12)}$$

The condition for the reverse transformation is assumed to be as

$$\tau = \tau_M - \tau_C, \qquad \text{(Eq 13)}$$

where τ_C is a material constant. By treating that the reorientation of martensite variants will occur when the maximum resolved shear stress in a transformation system of a sub-element becomes larger by a certain amount than that of the already transformed system in the same sub-element, the reorientation condition can be written as

$$\tau = \tau_M \quad \text{and} \quad \tau \geq \tau(M) + \tau_{OR}, \qquad \text{(Eq 14)}$$

where $\tau(M)$ denotes the resolved shear stress on the already transformed plane and τ_{OR} is a material constant.

2.6 Temperature Dependency of Critical Stresses for Transformation

In order to analyze the behavior of shape memory alloys under various mechanical and thermal loadings, it is necessary to give the temperature dependency of the critical stresses. Because of the lack of experimental data, the linear and parallel

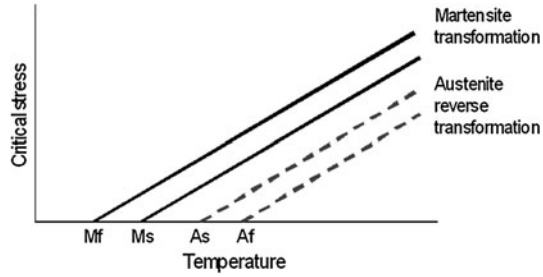

Fig. 3 Temperature dependency of critical stresses for transformation

relations between temperature and critical stresses are assumed as shown in Fig. 3, where M_s, M_f , A_s and A_f denote the martensite start temperature, the martensite finish temperature, the reverse transformation start temperature, and the reverse transformation finish temperature respectively. The value of the martensite transformation stress τ_M of ith sub-element of a crystal grain at a temperature is set to be a value between martensite start stress τ_{Ms} and the martensite finish stress τ_{Mf} at the temperature as

$$\tau_M = \tau_{Ms} + (\tau_{Mf} - \tau_{Ms})\frac{i-1}{N} \quad (i = 1 \sim N+1), \qquad \text{(Eq 15)}$$

where N is the division number of a crystal grain to sub-elements. Equation 15 means that the linear hardening property of transformation of a crystal grain is assumed and equal volume fractions of sub-elements are also assumed indirectly. The linear hardening assumption is not necessarily correct. But the main hardening property observed in the stress-strain curve of the material is represented by redistribution behavior of the stress in the polycrystalline material. Thus the influence of the linear hardening of the crystal grain or the nonlinear hardening is not serious with polycrystalline material. It is postulated that the same relation holds for τ_{OR}, namely,

$$\tau_{OR} = \tau_{OR1} + (\tau_{Mf} - \tau_{Ms})\frac{i-1}{N} \quad (i = 1 \sim N+1) \qquad \text{(Eq 16)}$$

2.7 Condition for Plastic Deformation (Ref 7)

The plastic strain can be also described by the constitutive model mentioned above. When the maximum resolved shear stress τ of slip planes in each crystal grain arrives at the critical value τ_y (the yield stress), the plastic shear strain shall occur in the direction of the stress. The yield condition is written as

$$\tau = \tau_y \qquad \text{(Eq 17)}$$

The temperature dependency of the yield stress and the strain hardening properties are not considered here for simplicity. The magnitude of the plastic strain increment is controlled by the restriction of the surrounding grains. This situation is satisfied by applying the equal strain model shown in Fig. 1. For the present calculation, the slip planes are assumed to be the same as the transformation planes. Though there are other slip planes too in the body centered cubic crystal of shape memory alloys, the calculations are carried out with considerably high flexibility of the plastic deformation and it is thought that the result shows a basic characteristic of the plastic deformation.

2.8 Interaction of Transformation and Plastic Strain

It is recognized by the experiment that plastic strain causes the degradation of transformation stress or the increase of the transformation temperature. The degradation of the transformation stress depending on the plastic strain is explained phenomenologically by introducing the effect that the plastic strain in a slip system which is the same as the transformation system causes the degradation of the transformation stress in the same direction by an amount in proportion to the quantity of the plastic strain.

To express the degradation of the transformation stress in the calculation, the conditions for the transformation expressed as Eq 12 and 13 are changed into as

$$\tau = \tau_M - p \times \gamma_p \quad \text{(Eq 18)}$$

$$\tau = \tau_M - \tau_C - p \times \gamma_p, \quad \text{(Eq 19)}$$

where γ_p denotes the plastic strain, and p is a material constant given tentatively as

$$p = E_m/10, \quad \text{(Eq 20)}$$

where E_m is Young's modulus of martensite.

3. Sample Calculations

To demonstrate the validity of the constitutive model, sample calculations are conducted.

3.1 Material Constants

Some of the material constants (E_a, E_m, τ_{ms}, τ_{mf}) are obtained from experimental data of Ti-Ni wires at 333 K. Martensite start temperature M_s is obtained from the differential scanning calorimetry (DSC) data of the material. Remaining constants necessary for the analysis are tentatively determined only for calculation purpose. Material constants used in the present calculations are listed and shown in Table 1.

Table 1 Material constants for sample calculations

Young's modulus of austenite	E_a = 65.5 GPa
Young's modulus of martensite	E_m = 14.1 GPa
Poisson's ratio	ν = 0.3
Martensite start stress (333 K)	τ_{ms} = 151 MPa
Martensite finish stress (333 K)	τ_{mf} = 155 MPa
Constant for reverse transformation	τ_C = 50 MPa
Constant for reorientation	τ_{OR1} = 30 MPa
Yield stress	τ_y = 300 MPa
Martensite start temperature	M_s = 282 K
Coefficient of plastic strain for interaction effect	p = 1.41 GPa

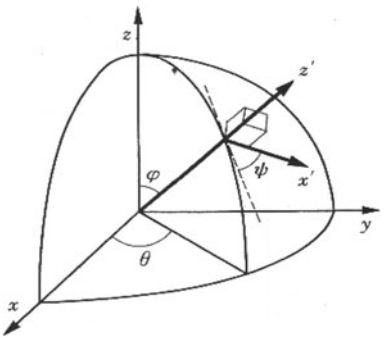

Fig. 4 Euler angle

3.2 Calculation Procedure

The crystal orientations of micrograins are described with Euler angles shown in Fig. 4. Considering the symmetry of the crystal structure, only angles between 0 and $\pi/2$ are considered in ϕ, θ, and ψ. Euler angles are divided by 6 in ϕ, 3 in θ, and 3 in ψ, respectively, for numerical computations in the present case, and total 54 micrograins of different crystal orientation constitute a material point. In the present calculation, the division number N of a grain for sub-elements is set to be 1000. Numerical calculations are conducted through an incremental method by a strain control procedure and the magnitude of an increment is employed to cause the transformation at one transformation system.

3.3 Superelastic Behavior with Plastic Strain Effect

Calculated results for the superelastic behavior at 333 K are shown in Fig. 5. In the small strain range the typical superelastic behavior is shown in the figure. At larger strain range, the plastic strain occurs and the residual strain can be seen at zero stress. And the interaction effect that the plastic strain causes the degradation of the reverse transformation

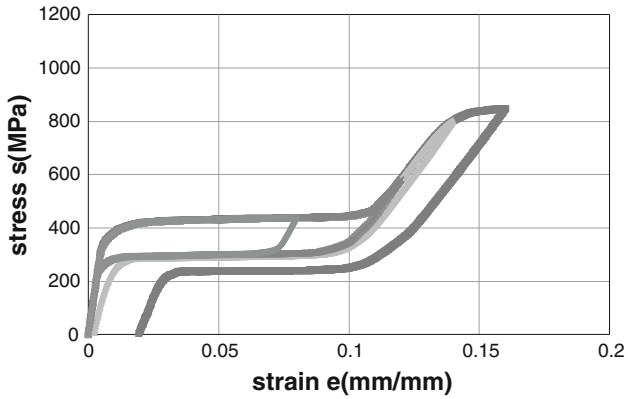

Fig. 5 Uniaxial stress-strain curve under uniaxial loading and unloading considering elastic, transformation, plastic strain and their interaction

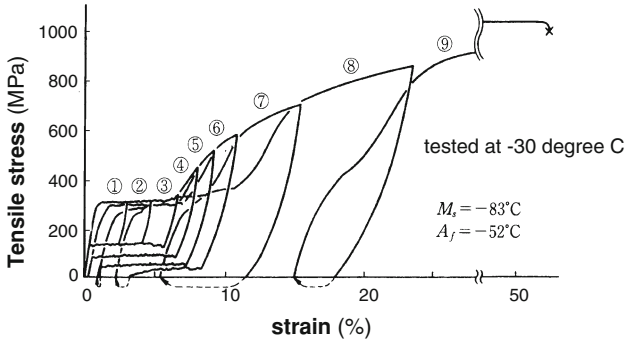

Fig. 6 Experimental stress-strain curve for superelastic Ti-Ni alloy (Ref 10, p. 45)

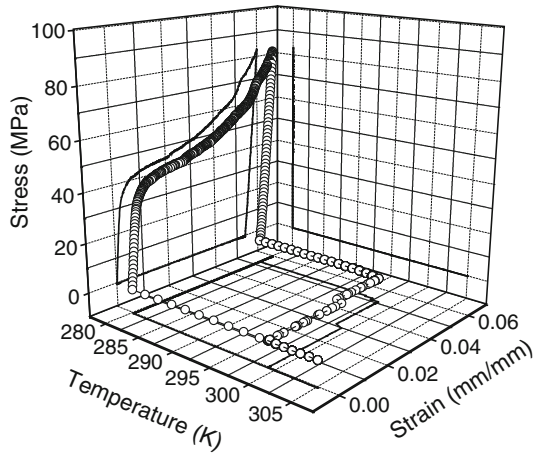

Fig. 7 Calculated results for the shape memory effect

stress is successfully represented in the figure. These results are reasonable in comparison with the experimental data shown in Fig. 6 (Ref 10, p. 45). The experimental data shown in Fig. 6 were provided in the material which was different from the material used for obtaining material constants in Table 1. Thus the comparison between Fig. 5 and 6 has only a qualitative meaning. And the size and the number of crystal grains within the cross-sectional area of the wire are not subject of concern because calculations in the present paper are limited to show the applicability of the constitutive model in the cases of uniaxial stress states and not in the case of actual thin wires. When the deformation behavior of actual thin wires is calculated, it should be necessary to investigate the interaction effect of small number of crystal grains in the small cross-sectional area and also the effect of the surface of the specimens.

3.4 Shape Memory Effect

Figure 7 shows the three-dimensional plots for calculated results for the shape memory effect. The initial conditions are $\sigma = 0\,\text{MPa}$, $\varepsilon = 0\%$, and $T = 280\,\text{K}$ which is the temperature below the martensite finish temperature. The distribution of martensite variants at the initial conditions is calculated beforehand in the temperature decreasing process from the temperature higher than the reverse transformation finish temperature to the temperature lower than the martensite finish temperature. In this calculation process, the normal component of the intrinsic transformation strains (see Eq 10) becomes important. The normal component of the intrinsic transformation has the great role on the accommodation behavior of shape memory alloys in the case of the thermal-induced transformation under stress-free conditions (Ref 6). In the loading process of $\varepsilon = 0\% \rightarrow 6\%$ at $T = 280\,\text{K}$, the transformation behavior by the reorientation of martensite variants is depicted in Fig. 7. In the unloading process at $T = 280\,\text{K}$, the elastic behavior is shown with residual strain at zero stress, and this residual strain gradually disappears under the stress-free condition with increasing of the temperature of $T = 280\,\text{K} \rightarrow 305\,\text{K}$ which is the temperature higher than the reverse transformation finish temperature. Thus the shape memory effect is calculated. A jump is shown in the temperature-strain curve. But, this is due to the poor resolution of the 3-D plotting machine. The smooth response is obtained in the fine resolution plot. Figure 8 shows

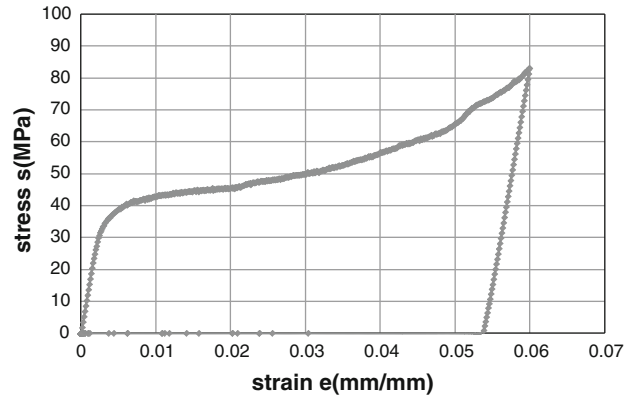

(a) Stress-Strain Relations

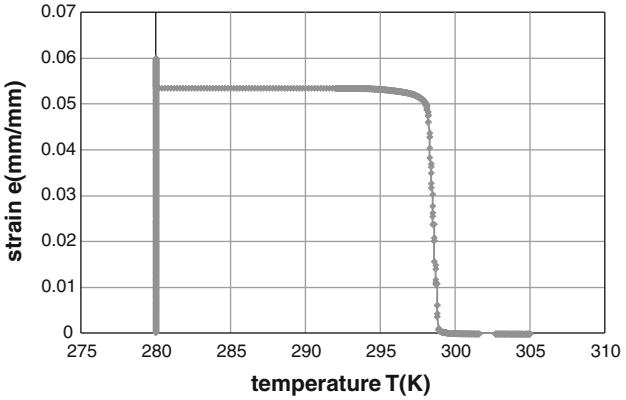

(b) Strain-Temperature Relations

Fig. 8 Two-dimensional plots for the shape memory effect

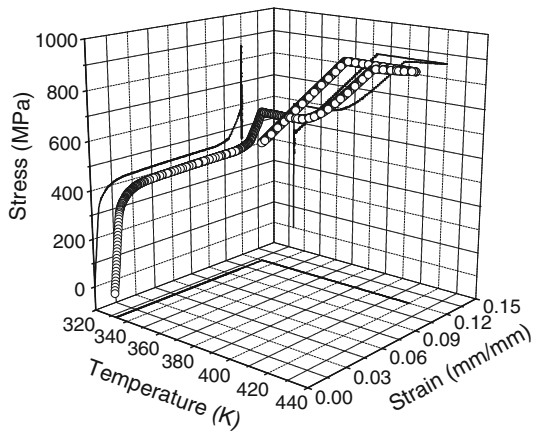

Fig. 9 Behavior for temperature change with strain holding

the two-dimensional plots of the same results. Smooth relations are obtained between strain and temperature showing the shape memory effect.

3.5 Behavior for Temperature Change with Strain Holding

Figure 9 shows the stress response for temperature change of $T = 333\,\text{K} \rightarrow 420\,\text{K} \rightarrow 333\,\text{K}$ with strain holding at $\varepsilon = 12\%$. The stress rise with the temperature increase is

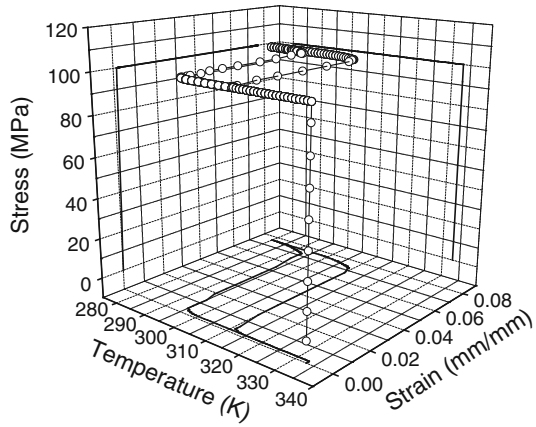

Fig. 10 Behavior for temperature change with stress holding

shown in the figure. This is because the critical stress for the transformation becomes large according to the temperature increase. This figure also shows the stress may rise as high as that causes the plastic deformation in the strain-arrested structure.

3.6 Behavior for Temperature Change with Stress Holding

Figure 10 shows the strain response for the temperature change of $T = 333\,\mathrm{K} \rightarrow 280\,\mathrm{K} \rightarrow 333\,\mathrm{K}$ with stress holding of $\sigma = 100\,\mathrm{MPa}$. The strain variation with the temperature change at a constant stress is depicted and a hysteresis loop is shown in the projection on the temperature-strain plane. This figure may be useful in understanding the response of the SMA actuator acting under constant loading.

3.7 Response of SMA Wire Structure with Bias Spring

Figure 11 shows a wire structure of SMA with a bias spring fixed at both ends. This structure represents the simplest device modeling a SMA actuator. The controlling equation of this problem can be obtained as follows. Consider an equilibrium state of the SMA wire and the bias spring in the structure shown in Fig. 11 at a described temperature. The stress and the strain acting on the SMA wire are denoted as σ^0 and ε^0, respectively. When a change in the temperature occurs, the stress and the strain also change. Their values are denoted as σ and ε, respectively. The force F acting on the spring is written as

$$F = A\sigma^0 - k(\varepsilon - \varepsilon^0)l, \qquad \text{(Eq 15)}$$

where A, k, and l are the area of the cross section of the SMA wire, the spring constant of the bias spring, and the length of the SMA wire, respectively. As this force is also acting on the SMA wire, the stress σ and the strain ε of the SMA wire is written as

$$\sigma = \frac{1}{A}\left\{A\sigma^0 - k(\varepsilon - \varepsilon^0)l\right\} = \sigma^0 - K(\varepsilon - \varepsilon^0) \qquad \text{(Eq 16)}$$

$$\varepsilon = \frac{1}{\hat{E}}\left\{\sigma^0 - K(\varepsilon - \varepsilon^0)\right\} + \varepsilon^{\mathrm{tr}} \qquad \text{(Eq 17)}$$

$$K = \frac{kl}{A}, \qquad \text{(Eq 18)}$$

where $\hat{E}$ is the average elastic modulus of the polycrystalline SMA wire with the mixture of austenite phase and martensite

Fig. 11 SMA wire structure with bias spring

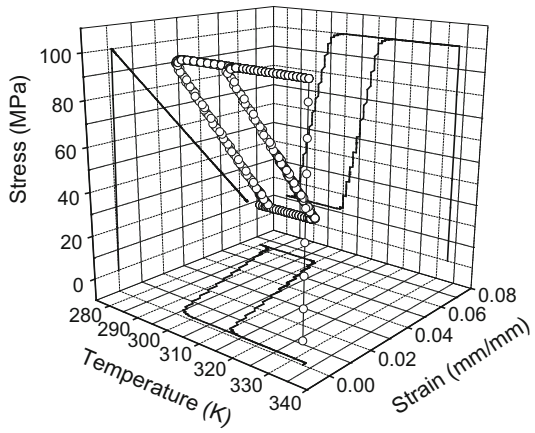

Fig. 12 Response of SMA wire structure with bias spring

phase, and $\varepsilon^{\mathrm{tr}}$ is the transformation strain. From Eq 17, the strain ε of the SMA wire is written as

$$\varepsilon = \left(\frac{1}{\hat{E}}\sigma^0 + \frac{K}{\hat{E}}\varepsilon^0 + \varepsilon^{\mathrm{tr}}\right) \Big/ \left(1 + \frac{K}{\hat{E}}\right) \qquad \text{(Eq 19)}$$

The several values of K are adopted for sample calculations. Results for the case of $K = 1.41\,\mathrm{GPa}\ (= E_{\mathrm{m}}/10)$ are shown in Fig. 12. Some convergence procedure is needed to obtain numerical results of Eq 16 and 19. Loading paths are as follows:

initial state: $T = 333\,\mathrm{K}$, $\sigma = 0\,\mathrm{MPa}$, $\varepsilon = 0\%$
path1: $T = 333\,\mathrm{K}$, $\sigma = 0\,\mathrm{MPa} \rightarrow 100\,\mathrm{MPa}$ The both ends of the structure are fixed at the end of the path.
path2: $T = 333\,\mathrm{K} \rightarrow 280\,\mathrm{K}$
path3: $T = 280\,\mathrm{K} \rightarrow 333\,\mathrm{K}$

Figure 12 shows the response of the structure in the space of stress, strain, and temperature. The stress behavior with the temperature change is shown in the projection on the temperature-stress plane. This figure shows the performance of the device as an actuator. And the strain behavior with the temperature change in the projection on the temperature-strain plane shows that the device can also be available to a temperature-driven position control system.

4. Conclusions

A constitutive model is proposed to describe the accommodation mechanism in the transformation behavior of shape memory alloys. The proposed constitutive model can predict the transformation behavior including the plastic strain effect of polycrystalline Ti-Ni shape memory alloys under various thermal and mechanical loading conditions. To demonstrate the validity of the constitutive model, sample calculations are

conducted. Though the model is applicable to the case of the multiaxial stress and strain, results of sample calculations presented in the present paper are only for the uniaxial stress and strain. Results for the multiaxial stress state will be presented in the near future. Calculated results are given for the superelastic behavior including the effect of the plastic strain, the shape memory effect, the transformation behavior under temperature change with stress or strain holding, and the structural behavior of a shape memory wire with a bias spring. This structure is the simplest model for SMA actuator driven by thermal loading. As shown in Fig. 5-12, calculated results are considered to be reasonable qualitatively. The applicability of the proposed constitutive model to the deformation behaviors of shape memory alloys under complex loading conditions of stress-strain and temperature is thus proved. But discussions are made only qualitatively because some of material constants used in the calculation are not determined by the data obtained experimentally. As the model is constructed in the micromechanical framework, the material data necessary for the calculation are those of the microstructure of the material. It is very difficult to obtain such data directly by macroscopic experiments. Some indirect way may be required to determine the material constant of the microstructure using the macroscopic experimental data of the material. Discussions on how to obtain the material constants and the quantitative evaluation by a direct comparison between calculations and experiments are left to the future work.

References

1. K. Tanaka, H. Tobushi, and S. Miyazaki, *Mechanical Properties of Shape Memory Alloys*, 1st ed., Yokendo, Tokyo, 1993, p 62–122
2. M. Tokuda, Y. Men, B. Bundara, and P. Sittner, Multi-axial Constitutive Equations of Polycrystalline Shape Memory Alloy (1st Report, Modeling and Formulation), *Trans. JSME, A*, 1999, **65–631**, p 491–497
3. L.C. Brinson, One-Dimensional Constitutive Behavior of Shape Memory Alloys : Thermomechanical Derivation with Non-Constant Material Functions and Redefined Martensite Internal Variable, *J. Intell. Mater. Syst. Struct.*, 1993, **4**, p 229–242
4. M. Panico and L.C. Brinson, A Three-Dimensional Phenomenological Model for Martensite Reorientation in Shape Memory Alloys, *J. Mech. Phys. Solids*, 2007, **55**, p 2491–2511
5. H. Cho, A. Suzuki, and T. Sakuma, Interaction Surface of Phase Transformation Stress by Constitutive Model for Accommodation of Transformation Strain, *Trans. MRS-J*, 2010, **35**(2), p 359–363
6. H. Cho, A. Suzuki, T. Yamamoto, Y. Takeda, and T. Sakuma, Numerical Investigations for Thermally Induced Transformation, Reorientation of Martensite Variants and Shape Memory Effect of Shape Memory Alloys using Constitutive Model for Accommodation of Transformation Strain, *Mater. Sci. Forum*, 2011, **687**, p 510–518
7. H. Cho, A. Suzuki, T. Yamamoto, and T. Sakuma, Influence of Plastic Strain on Transformation Behavior of Shape Memory Alloys, *Trans. Mater. Res. Soc. Jpn.*, 2011, **36**(3), p 441–444
8. A. Suzuki, A Modified Fraction Model for the Viscoplastic Behavior of Metals, *Proceedings of the International Conference on Creep '86*, 1986, p 471–476
9. G.I. Taylor, Plastic Strain in Metals, *J. Inst. Met.*, 1938, **62**(307–324), p 307–324
10. K. Tanaka, H. Tobushi, and S. Miyazaki, *Properties of Shape Memory Alloys*, 1st ed. Yokendo, Tokyo, 1993, p 86, 94